Lab on a Chip

Accepted Manuscript

RSC Publishing

www.rsc.org/loc
Registered Charity Number 207890

Integrated microspectrometer for fluorescence based analysis in a microfluidic format

Zhixiong Hu[1], Andrew Glidle[1], Charles N. Ironside[1], Marc Sorel[1], Michael J. Strain[1], Jon Cooper[1], Huabing Yin[1*]

[1] *School of Engineering, University of Glasgow, G12 8LT Glasgow, U.K.*

**Email : Huabing.Yin@glasgow.ac.uk, tel : +441413304109*

We developed an Arrayed Waveguide Grating (AWG) microspectrometer integrated with microfluidics to perform spectroscopic fluorescence measurements as used in biological assays.

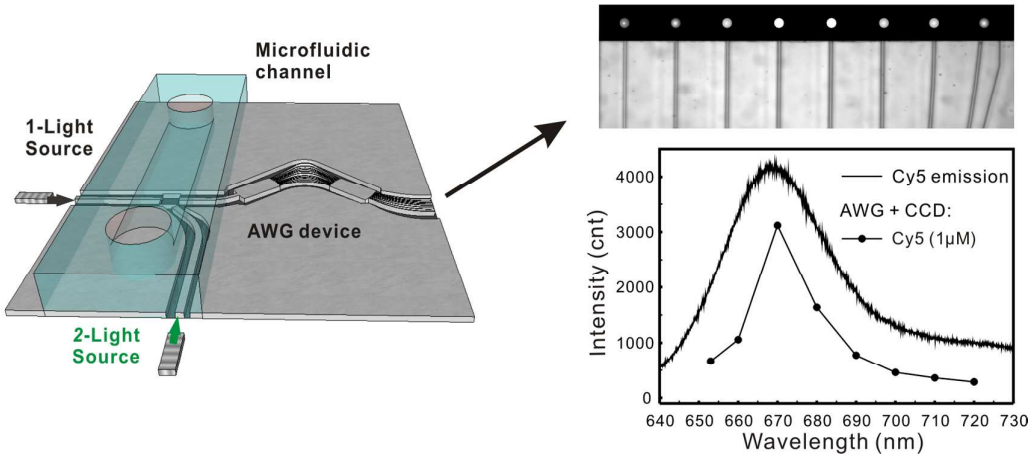

Cite this: DOI: 10.1039/c0xx00000x

www.rsc.org/xxxxxx

ARTICLE TYPE

Integrated microspectrometer for fluorescence based analysis in a microfluidic format

Zhixiong Hu, Andrew Glidle, Charles N. Ironside, Marc Sorel, Michael J. Strain, Jon Cooper, and Huabing Yin*

Received (in XXX, XXX) Xth XXXXXXXXX 20XX, Accepted Xth XXXXXXXXX 20XX
DOI: 10.1039/b000000x

We have demonstrated a monolithic integrated Arrayed Waveguide Grating (AWG) microspectrometer–microfluidic platform capable of fluorescence spectroscopic analysis. The microspectrometer in this proof of concept study has a small (1 cm x 1 cm) footprint and 8 output channels centred on different wavelengths. We show that the signals from the output channels detected on a camera chip can be used to re-create the complete fluorescence spectrum of an analyte. By making fluorescence measurements of (i) mixed quantum dot solutions, (ii) an organic fluorophore (Cy5) and (iii) the propidium iodide (PI)-DNA assay, we illustrate the unique advantages of the AWG platform for simultaneous, quantitative multiplex detection and its capability to detect small spectroscopic shifts. Although the current system is designed for fluorescence spectroscopic analysis, in principle, it can be implemented for other types of analysis, such as Raman spectroscopy. Fabricated using established semiconductor industry methods, this miniaturized platform holds great potential to create a handheld, low cost biosensor with versatile detection capability.

INTRODUCTION

Rapid, on-site detection of samples has become important in many fields as a result of growing needs in diagnostics, environmental monitoring, food safety, and homeland security. These emerging demands have driven the rapid development of portable biosensors and lab-on-a-chip devices designed to analyse materials in samples that range from clinical swabs to pathogenic bacteria[1-6]. Since the majority of targeted analytes are present in minute quantities and often within a complex matrix, high selectivity, sensitivity and accuracy are of paramount importance for a detection method. In this context, fluorescence based approaches are amongst the most highly developed, widely applied, optical assay techniques. It is no surprise that conventional fluorescence microscopy is commonly used in biological labs. However, fluorescence microscopes are bulky and require either discrete filter sets to separate fluorescence from excitation light or an equally bulky conventional spectrometer. This makes the instrumentation for 'simultaneous' detection of more than 2~3 analytes highly challenging (and expensive).

Various approaches towards miniaturisation of fluorescence detection on chip have emerged in recent decades in which micro-optical functionalities are integrated with microfluidic (and lab-on-a-chip) devices [7-10]. A few devices have been constructed with on-chip integration of components such as light sources, light guides (i.e. waveguides), and detectors (e.g. photodiodes)[11-13]. However, their moderate detection sensitivity as well as demanding fabrication procedures remain challenges to be addressed. Currently, the typical approach for performing fluorescence measurements in a microsystem is to interface it with external systems such as light sources, filters and/or detectors.

The filtering function of a fluorescence sensing system is one of the most critical determinants of its sensitivity and selectivity. The basic requirement for a filtering device in fluorescence is that it should attenuate the excitation light sufficiently but transmit light at specific fluorescence wavelengths, largely unattenuated. Typically in a bench-top set-up (e.g. a plate reader or scanner) this is done using fixed colour or interference filters. In striving for miniaturisation, several efforts have focused on the integration of filtering functions on chip [2, 7, 14-16]. A comprehensive review of various filtering techniques that could be employed, including those based on interference, absorbance and waveguide gratings is given by Dandin et al [7] and some monolithic integration of these components with microfluidic devices has been recently reported [2, 7, 14-18]. A drawback to these techniques is that individual chips are fabricated with designs that are appropriate to work in a wavelength range specific to a particular fluorophore or chromophore. This means that if, for example, the fluorophore is changed during the course of an investigation, a different chip must be designed, fabricated and used. Modification of such bespoke designs represents an even greater challenge in measurements involving multiple fluorophores or chromophores.

Cite this: DOI: 10.1039/c0xx00000x

www.rsc.org/xxxxxx

ARTICLE TYPE View Online

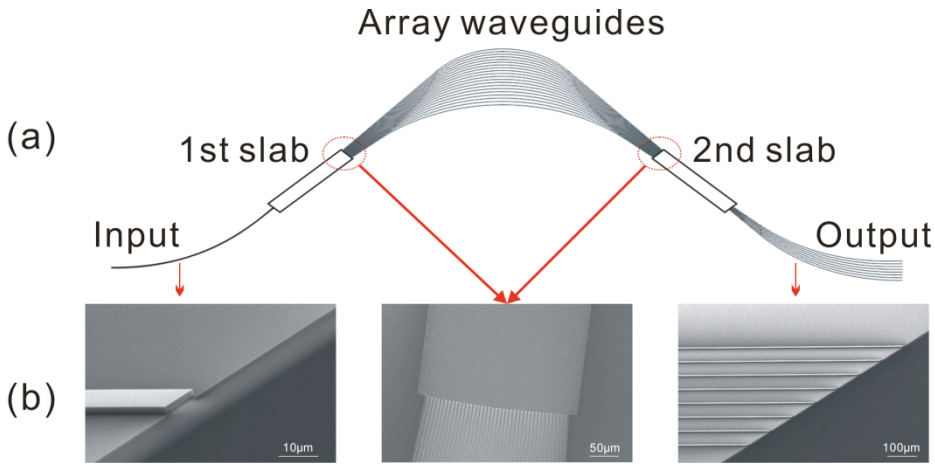

Fig. 1 (a) Configuration of an AWG device. A typical AWG device comprises: input waveguide, 1st slab region, arrayed waveguides, 2nd slab region and output waveguides. (b) SEM images of representative units of the fabricated eight channel AWG. Left, the input; Middle, the interface between the 1st slab (and the 2nd slab) with the arrays of single mode waveguide, and Right, the eight output channels. The arrows indicate their corresponding positions in the AWG device.

As an alternative to measuring fluorescence with band pass filters, spectral discrimination of different wavelengths using a grating or prism type of spectrometer offers excellent versatility [7]. At the macroscopic scale, *spectroscopic* analysis (e.g. fluorescence, Raman, IR spectroscopy) has been well established for a vast range of applications. For example fluorescence *spectroscopy* is widely used in the detection of environmental polyaromatic pollutants [19] and explosives [20]. Currently, the compact spectroscopic systems commercially available are based on free space optical systems and folding of the light path. Further miniaturisation of these systems is difficult. In the last decade there has been development of several different microscopic spectrometer chip formats. The methodologies employed have been based on waveguide gratings [21-24], planar photonic crystals [25] and narrow band arrayed waveguide (AWG) designs. Some of these systems have been successfully used to perform absorbance-based measurements [11, 24-26]. However, the implementation of on chip microspectrometers for fluorescence based analysis is in its very early stages, as evidenced by the small number of publications [21].

Here, we report the development, for the first time, of a monolithic integrated Arrayed Waveguide Grating (AWG) microspectrometer–microfluidic platform capable of fluorescence spectroscopic analysis. As will be described in detail below, an AWG device is one in which a series (array) of waveguides of slightly different optical path lengths are used to separate 'white' light into its component wavelengths in a manner similar to the combination of a prism and an interference filter.

AWGs are one of the most important, highly integrated spectrometer approaches in current optical systems associated with the telecomm's industry. They are extensively used in the near infrared wavelength range (between 1.3μm and 1.6μm) as optical (de)multiplexers[27, 28]. As a result of the advanced, high volume, fabrication techniques associated with this industry, the possibility of employing an on-chip AWG spectrometer for biological and chemical sensing applications offers the prospects of realising genuinely integrated, light weight instruments with high performance and low cost. However useful spectroscopic characteristics for aqueous biological and chemical samples mostly occur in the visible wavelength range. Thus designing and developing a visible AWG (i.e. an AWG for the visible wavelength range) is essential to exploit this technology. In the last few years, several visible AWG microspectrometers capable of absorbance measurements have been demonstrated [26, 29-31]. However, the use of AWG technology for fluorescence measurements either alone or in an integrated device has not been explored.

In the report below, we begin with a description of the design and fabrication of the visible AWG microspectrometer, followed by its characterisation and integration with microfluidic devices. We then interface the platform with an external light source and an imaging detector to evaluate its capability for fluorescence based analysis. The versatility of the platform is shown by making fluorescence measurements of mixed quantum dot solutions, an organic fluorophore (Cy5) and the propidium iodide (PI)-DNA assay. We illustrate the unique advantages of the AWG configuration for simultaneous, quantitative multiplex detection and its capability in the detection of small spectroscopic shifts, as in an assay system.

RESULTS AND DISCUSSION

Fluorescence AWG microspectrometer design

To fabricate a visible AWG spectrometer, the prime requirement is that its component materials should have high transparency at

visible wavelengths. Such materials include silica, silicon-oxynitride and a range of polymers. In this work, flame hydrolysis deposited (FHD) silica was used to fabricate a visible AWG device, since modulation of the refractive index of FHD can be well controlled by dopant incorporation during its growth, densification, or ion implantation.

The visible AWG device in this work was designed with a centre wavelength (λ_c) of 680nm and channel-channel wavelength spacing ($\Delta\lambda$) of 10nm. The configuration of the AWG is as shown in Figure 1(a), comprising 5 units, namely, 1) the input waveguide, 2) the 1st slab region, 3) the arrayed waveguides, 4) the 2nd slab region, and 5) the output waveguides. Light coupled into the input waveguide traverses to the 1st slab region and then enters the arrayed waveguides. The optical path length of the waveguides is linearly varied across the array by variation of the geometrical length of each waveguide. This results in a phase shift between light exiting from the different channels, leading to interference in the following free-space/slab region. The output waveguides are located on the opposite side of the free-space/slab region in positions where maxima in the interference pattern occur.

Considering single-mode operation and based on a 1.5% refractive index contrast between the waveguide core and the underlayer, the dimensions for a single-mode waveguide core were designed to be 2 μm width by 2 μm thickness. In contrast to conventional NIR AWG devices, both the input and output waveguides were designed to be larger (width 8 μm) in order to enhance light collection, although this comes at the expense of spectroscopic resolution.

AWG device fabrication and characterisation

In this prototype development work, photo- and electron beam-lithography were employed to define the AWG pattern, with Reactive Ion Etching being used for deep etching of the FHD silica. Figure 1b shows representative SEM images of the fabricated 8 channel AWG. It is clear that all the waveguides have well defined sidewalls and corners. The well defined sidewalls and corners of the waveguides seen in Figure 1 result in reproducible device-device performance in accordance with simulations (see below) and minimal scattering losses. The height of all the waveguides, the width of the arrayed waveguides and the width of the input/output waveguides are 1.99 μm, 2.32 μm and 7.78 μm respectively, which are close to the designed value (i.e. 2 μm × 8 μm) . The overall dimensions between the two slab regions of the AWG device are ~5 mm length by ~1.5 mm width (Figure 2a). The transmission spectrum of each channel in the fabricated AWG device is shown in Figure 2b. The Full Width at Half Maxium (FWHM) of each output peak is ~10 nm, consistent with simulations obtained using 3D BeamPROP software (Rsoft Ltd) (data not shown).

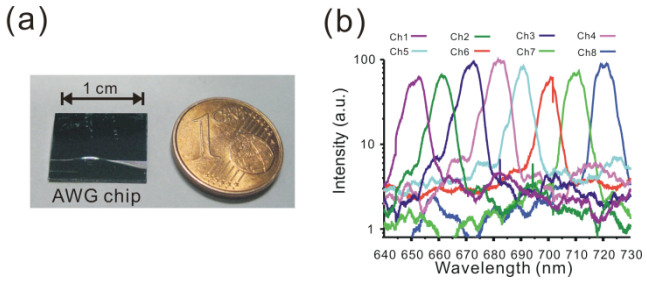

Fig. 2 (a) A picture of an 8 channel AWG chip. (b) Experimental transmission spectrum of the AWG device. Intensities scaled so that the maximum transmission equals 100 arbitrary units. Different colours indicate signals from each output channel.

Integration of the AWG- microfluidic platform

A significant advantage of employing well established microfabrication processes in this work is that it allows monolithic integration of the AWG device with other functional components, including optical guiding systems and microfluidic networks for sample handling. Currently, microfluidics oriented spectroscopic analyses usually employ standalone optical components, such as optical fibres and objective lenses, to integrate spectrometers and light sources with a microfluidic system [32, 33]. With these latter systems, detection of signals is heavily dependent on mechanical optical alignment and so subject to errors and variability, aside from being time consuming. In contrast, monolithic integration permits micro- and nano-scale level alignment of multiple functional components on a single chip, and is amenable to mass production.

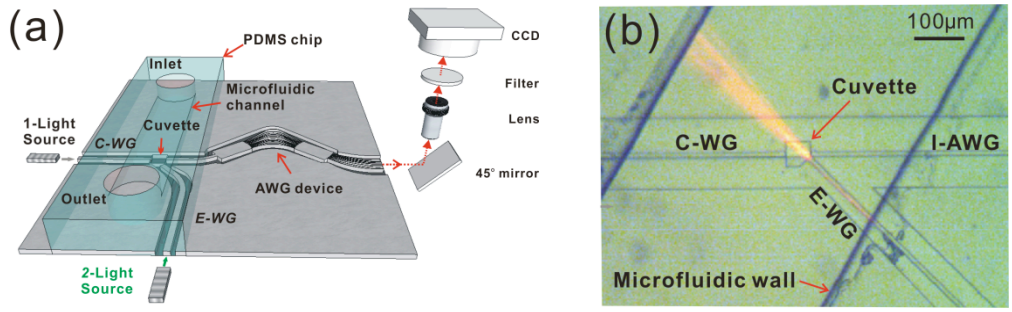

Fig. 3 (a) Schematic illustration of integration of AWG device with microfluidics and CCD. A 45° mirror and a ×4 objective lens were used to reflect AWG output signals onto a vertically mounted CCD camera or a photon detector.. (b) A close up view of a monolithic integrated AWG- PDMS microfluidic chip, where the sampling cuvette is located in the middle of the microfluidic channel. The white flare starting in the cuvette area and going diagonally towards the top left of the microfluidic channel shows the path of light emanating from the excitation waveguide. C-WG: white light characterisation waveguide. E-WG: excitation waveguide. I-AWG: AWG input waveguide.

As schematically shown in Figure 3a, the monolithic integrated AWG- microfluidic platform contains three units: 1) light source waveguides, 2) sampling region (Note: this can be part of a microfluidic network), and 3) an AWG device. The initial design

of the sampling region consists of a square shaped cuvette located at the junction of the light source waveguides and the AWG input waveguide. The white light source waveguide (C-WG in Figure 3a) crosses the centre of the sample cuvette and extends to the AWG input waveguide in a straight line. This allows characterisation of the AWG transmission spectrum and can also be used for absorbance analysis. The off-axis waveguide (E-WG, Figure 3a) is used to provide the excitation light in a fluorescence measurement. It intercepts the sample cuvette at an angle of 45° to the AWG input guide axis, to reduce the amount of excitation light entering the AWG, (in a fluorescence measurement the excitation light intensity is typically 3-4 orders of magnitude greater than that of the emitted light). The sample cuvette was 2 μm deep with length x width dimensions of either 100 μm x 100 μm for quantum dots measurements or 50 μm x 50 μm for solution measurements. It functions as either a defined container for depositing samples in static analyses (as demonstrated in the section on quantum dots below) or as part of a monolithically integrated microfluidic network, as shown in Figure 3b.

For high spectroscopic resolution, a large number of output channels are needed. This is achievable thanks to the benefits of the small device footprint of the device and the robust fabrication approach used. Although we have limited ourselves to 8 output channels in this proof-of-concept work, the fabrication of 512 channel devices has been well established for uses in other fields [34, 35]. Since simultaneous measurement of the outputs was essential, an imaging detector (e.g. camera) was ideal to collect and process signals from the different channels simultaneously. The use of an imaging camera eliminated the need to physically connect individual channels to photodetectors e.g. via pigtailed fibres. For this proof of concept study, the output channels were imaged onto an Andor 885 iXon CCD camera when performing light intensity measurements or coupled into a conventional Triax 320 spectrometer (Jobin Yvon) when performing spectroscopic measurements to characterise the output signals from the AWG.

Evaluation of Fluorescence measurements

As a consequence of designing the AWG element to operate over the UV-vis-NIR range, the AWG-microfluidic device has the potential to measure a fluorescence spectra from multiple fluorophores. This capability was evaluated qualitatively and quantitatively using common fluorescence probes, namely quantum dots and Cy5 fluorophore, as well as a fluorescence based assay (i.e. propidium iodide - DNA bioassay), as detailed in the following sections.

Multiplexing measurements of quantum dots

Quantum dots are widely used as fluorescence probes due to their narrow emission bandwidth and long-term photostability as well as their suitability for surface functionalisation [37]. Several quantum dots can be excited using a single light source, making them good probes for simultaneous detection of multiple analytes. Due to the narrow bandwidth of a quantum dot's emission, emissions from multiple quantum dots can be detected simultaneously from the individually addressable output channels of the AWG.

To evaluate this capability, two quantum dots, namely QD655 and QD705 were used. The emission from QD655 (655 nm) and QD705 (705 nm) corresponded to the central wavelengths of channel 1 and channel 6 respectively. For the purpose of evaluating and validating the AWG's spectroscopic performance, the spectra from each output channel on the AWG device were characterised by fibre coupling individual output waveguides to the entrance slit of a conventional spectrometer (TRIAX320). Thus the emission spectra of solutions containing a) QD655 only, b) QD705 only and c) a mixture of QD655 and QD705 were measured from each of the output channels. Spectra measured off chip from the same solutions were used as references to verify the performance of the AWG.

As shown in Figure 4a & b, the signal from QD655 was only detected in channel 1 while that from QD705 only appeared in channel 6 (outputs from the other channels were at background levels). This indicates minimal cross talk between the channels. Importantly, the single peak spectra from both channels are in excellent agreement with their reference spectra obtained off chip (the black curves in Figure 4 a & b). For a mixture of QD655 and QD705, signals from both channels 1 and 6 were detected (Figure 4 c). However, as the spectroscopic measurement of these signals showed, the light emitted from these channels consisted of only a single peak corresponding to the individual QD655 or QD705 fluorophores (channel 1 and 6 respectively, Figure 4c). Adding the spectroscopic outputs from these channels together gives an envelope that compares well with the double peak spectrum obtained from an off-chip, bulk solution, measurement using a conventional spectrometer. This demonstrates the effective capability of the AWG device in the discrimination of wavelengths and opens up the possibility of assaying a sample containing multiple targets.

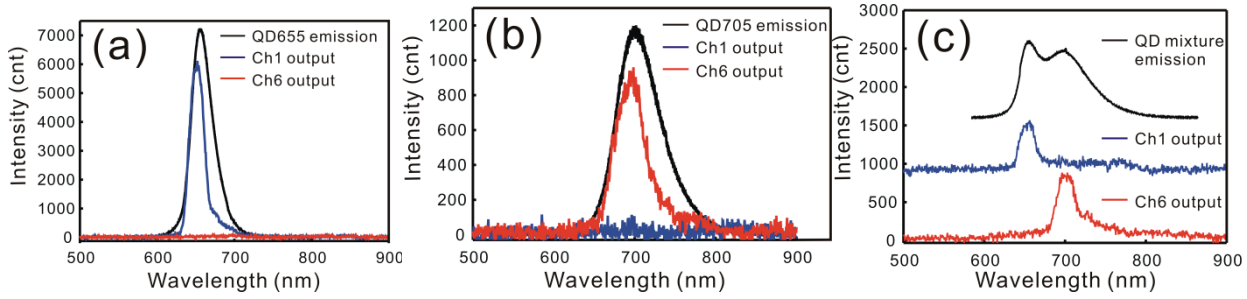

Fig. 4 Multiplexed measurement of quantum dots using the AWG device. Spectra of quantum dots in red and blue were obtained from the representative AWG output channel (1 & 6) while those in black were the corresponding references obtained via off chip measurement. Three solutions were used: (a) QD655 only, (b) QD705 only and (c) a mixture of QD655 and QD705.

Cite this: DOI: 10.1039/c0xx00000x

www.rsc.org/xxxxxx

ARTICLE TYPE View Online

Spectroscopic fluorescence measurements

Most current fluorescence sensing methods in which labelling is employed detect intensity variations at fixed wavelengths corresponding to the emission of the fluorophore of interest. However, a wide range of targets, such as explosives and toxins, can't easily be measured in this way due to issues associated with sample labelling. In addition, there are many substances and environmental conditions that can affect the photo-physical properties of a fluorophore, leading to subtle changes in both intensity and the shape of its spectrum [20, 38].

Enhancing fluorescence assays by incorporating spectroscopic measurements easily would significantly enlarge the application areas for a portable biosensor, especially in those situations that favour minimal human interactions. The suitability of the AWG-microfluidic platform for performing an accurate, quantitative, spectroscopic fluorescence measurement was evaluated by collecting the emission spectrum of Cy5 fluorophore using the set-up shown in Figure 2. Various Cy5 concentrations were delivered into the microfluidic channel at a flow rate of 6.7 mm/s. The spectrum from each channel was shown in Figure 5a. It is clear that, taken together, the peak intensities of the spectra collected from each of the 8 channels follow the shape of the complete Cy5 emission spectrum. Low crosstalk was again observed between each spectrum, demonstrating good fidelity of spectroscopic measurements by the AWG device.

With an understanding of, and confidence in, the output spectra from individual channels, a CCD camera was then employed to detect the light intensities from the output channels simultaneously. Figure 5b (i) shows a CCD image of the output from the 8 channels using a 1 μM Cy5 solution. The 8 bright spots correspond to the 8 output channels (Figure 5B (ii)). Plotting the intensities of the 8 spots from a CCD image versus their centre wavelengths (Figure 5B (iii)) clearly replicates the envelope of the Cy5 emission spectrum. Thus, the AWG device in conjunction with an imaging camera can provide a facile way to achieve a spectroscopic measurement. N.B. the measurements of the AWG output channels with a conventional spectrophotometer in Figure 5a demonstrate that the light spots at different positions on the CCD (Figure 5b) have wavelengths restricted to the corresponding AWG output channels.

Importantly, an increase of Cy5 concentrations resulted in a proportional increase in intensity on the CCD. This linear relationship is illustrated in Figure 6 where the intensity in the CCD image of an area corresponding to the output from a single example channel, channel 3, is integrated. Extensive efforts were not made to determine a limit of detection (LOD) for Cy5 fluorescence, however, the results obtained suggest this would be significantly lower than the lowest concentration (100 nM) measured. (The LOD would depend in part on the assay time and the excitation intensity). Together, the spectral resolution and linearity of the fluorescence-concentration plot demonstrate that the device is suitable for quantitative as well as qualitative fluorescence measurements. These capabilities offer new avenues for assays that involve detecting both intensity and shape of spectra, such as a propidium iodide (PI)-DNA assay (see below).

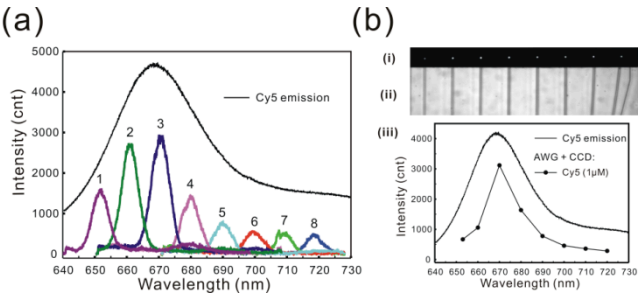

Fig. 5 Cy5 spectrum measurement using the AWG micro-spectrometer. (a) In conjunction with a conventional spectrometer to compare the spectra (colour lines) from the 8 output channels with the reference spectrum (the black line). (b) In conjunction with a CCD camera. (i) a CCD image of the output from Cy5 emission, channels from left to right are channel 1 to channel 8; (ii) top-down bright field image of the output waveguides; (iii) The plot of the 8 output intensities taken from a CCD image versus their central channel wavelength in comparison to a Cy5 emission spectrum.

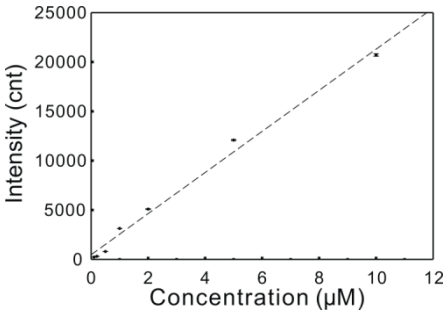

Fig. 6 The output intensities from channel 3 taken from CCD images at different Cy5 concentrations. The images were acquired for 5 minutes. Error bars indicate +/- one standard deviation.

Assays based on spectroscopic analysis

Propidium iodide (PI) is a fluorescence dye and intercalating agent, commonly used for quantitative analysis of DNA [39-41]. Once a PI molecule binds to DNA by intercalating between the bases, its fluorescence intensity is significantly enhanced and its peak emission exhibits a blue-shift. The variation in equilibrium concentrations of bound and unbound PI with increasing DNA concentration is complex. However, when using a PI solution of a given concentration, the amount of bound PI increases smoothly as the concentration of DNA increases until either all of the PI is bound, or the DNA is maximally loaded. Figure 7a shows the variations of fluorescence spectra collected using a conventional spectrometer from a 15 μM PI solution with a range of DNA concentrations and without DNA. As expected, the Stokes shifts

and increased intensity of the PI fluorescence spectra were observed in the presence of DNA.

The same PI-DNA solutions were then measured using the AWG-microfluidic device, interfaced to a CCD camera. As illustrated in Figure 7b, when PI is bound to DNA, the fluorescence intensities from the different channels recorded on the CCD increase. It is also observed that for the unbound PI solution the greatest intensity is on channel 8 (633 nm), corresponding to the low wavelength side of the 654 nm peak seen in Figure 7a. In contrast, when PI is bound to DNA, the greatest intensity in the CCD image is seen on channel 6 (614 nm) i.e. at the same wavelength as the peak position of the corresponding PI-DNA spectrum in Figure 7a. Thus the AWG response suggests the shift in wavelength between the fluorescence spectra of PI and PI-DNA.

In order to determine which channel has the greatest sensitivity for the detection of DNA bound to PI, the ratio of fluorescence intensities for bound and unbound PI was calculated for each channel. It was found that the relative increase in intensity is greatest at 570 nm (channel 1). Thus, in Figure 7c, the intensity from channel 1 is plotted against DNA concentration and compared with the corresponding intensities measured at 570 nm using a conventional spectrometer. Both plots are in excellent agreement, again validating the functionality of the AWG device and demonstrating the utility of being able to subtly adjust or select the particular wavelength range used in quantifying an assay so as to optimise a signal to background (e.g. blank) measurement.

It is worth noting that the above imaging based approach to evaluating a fluorescence spectrum, measures intensity patterns of all the outputs simultaneously, and thus enables detailed analysis of individual channels. This can be advantageous for more demanding analysis, for example in Förster resonance energy transfer (FRET) measurements and in quantitative ratiometric measurements, where variations at two or three wavelengths occur simultaneously.

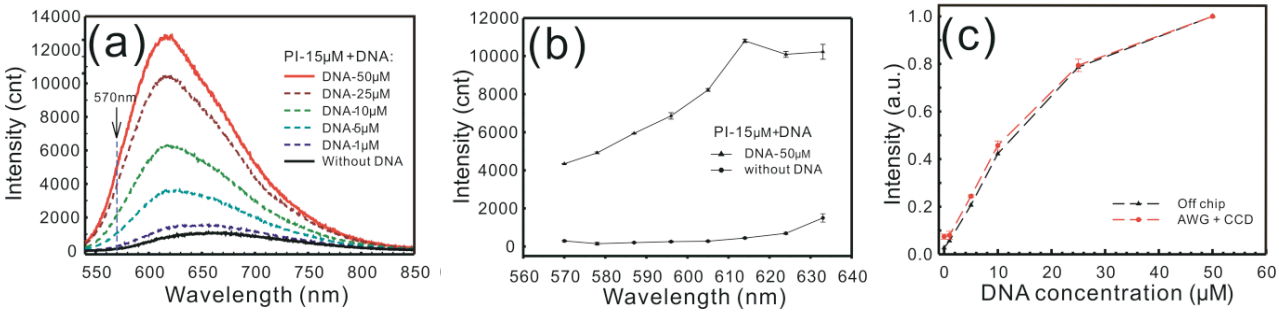

Fig. 7 (a) Fluorescence spectra of PI solutions with and without DNA (obtained off chip). (b) The intensity profile of the 8 outputs taken from CCD images for the same solutions used in (a). (c) Fluorescence intensity versus DNA concentrations plots comparing off chip spectrometer measurement (data taken from (a) at 570 nm) and on chip measurement with a CCD detector (data taken from channel 1). The images were acquired for 5 minutes. Error bars indicate +/- one standard deviation.

EXPERIMENTAL SECTION

Materials

Flame hydrolysis deposited (FHD) silica-on-silicon wafers (Gemfire Ltd) were used to fabricate the AWG device. By controlling the dopant level in the silica, the wafer can be manufactured with two layers of deposited silica having different refractive indices. The underlayer silica has thickness of 8 μm and refractive index of 1.456. The top silica layer has thickness of 2 μm and refractive index of 1.478.

Quantum dot QD655 (655 nm emission) and QD705 (705 nm emission) solutions were obtained from Invitrogen, and used as received. Cy5, Propidium Iodide (PI), and salmon sperm DNA were purchased from Sigma-Aldrich and made into aqueous solutions using deionised water (pH7, Millipore).

Fabrication process of the AWG device:

The profile of the FHD waveguide cross-section is presented in Figure 8a. First, the FHD silica-on-silicon wafer was thoroughly cleaned using Nanostrip, water, acetone and isopropanol, before commencing the lithographic processes. A 75 nm thick copy of the AWG design was patterned onto the wafer using S1805 photoresist (Shipley), NiCr evaporation and a standard lift-off process. The NiCr served as an effective protection mask for subsequent Reactive Ion Etching (RIE) of the top, doped, silica layer (i.e. to an etch depth of 2μm). This led to the formation of waveguide core with the designed AWG features. After etching, a 400 nm layer of hydrogen silsesquioxane (HSQ, Dow Corning) (Refractive index: n=1.37) was spun on top of the wafer and hard baked to form an over-cladding layer.

After HSQ deposition and baking, a second lithographic/RIE etching process similar to that above was carried out to incorporate other features in the AWG-microfluidic design, including, for example, the cuvette for sampling. Prior to this however, a 200 nm PECVD silica layer was deposited on top of the device in order to protect the HSQ layer during the subsequent lithographic processes. Scanning electron microscopy (S4700, Hitachi) and profilometry (DEKTAK, Veto Instruments Ltd) were used to examine the device after each fabrication step. An SEM picture of the waveguide cross-section is shown in the

Figure 8b where borders between different materials are highlighted with dashed lines.

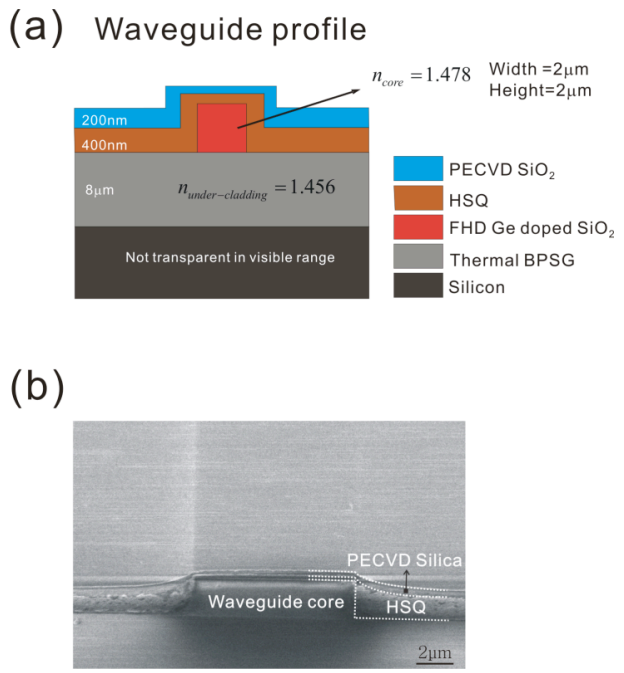

Fig. 8 (a) Schematic illustration and (b) SEM image of the cross section profile of the waveguide. The values of refractive indexes given correspond to those at a wavelength of 632.8 nm. BPSG: Boron-Phosphor-Silica-Glass.

Fabrication of PDMS chip and integration with the AWG device

A silicon master of a basic microfluidic channel (10 mm long x 500 μm wide x 100 μm high) was fabricated using standard photolithographic processes. The silicon master was silanised using trichloro(1H,1H,2H,2H-perfluorooctyl)silane (Sigma-Aldrich) prior to making the PDMS replicas. Polydimethylsiloxane (PDMS) (Sylgard 184 Silicone Elastomer, Dow Corning) was mixed at ratio 10:1 (base:initiator), degassed, cast on the master, and cured at 90° for 2 hours. The cured PDMS was then slowly pulled off the master and irreversibly bonded to an AWG chip via oxygen plasma treatment.

Spectral characterisation of AWG devices

To characterise the spectral range and throughput of each output channel a white light source (Anritsu MG922A) ranging from 400 to 1600 nm was coupled into the input waveguide of the AWG via a tapered optical fibre. A second tapered fibre was then aligned with each of the AWG output channels in turn, and connected to the entrance slit of a conventional spectrometer (TRIAX320, Jobin Yvon). Spectra were measured with typical acquisition times of <3 s. To aid alignment of the tapered fibres, the AWG-microfluidic device was mounted on the stage of an upright microscope to allow easy viewing of the fibres and light from a HeNe laser was injected into the non-tapered end of the fibre to indicate precisely whereabouts the light emanated from the tapered facet.

Fluorescence measurement using the AWG device-microfluidic platform

For the quantum dot measurements, to minimise the amount of material used, 2 μl of quantum dot solution was dropped in the cuvette of the AWG device and covered with a glass cover slip to prevent water evaporation. For the Cy5 and PI-DNA assays a range of concentrations (see text for details) were delivered into the microfluidic chip at a flow rate of 6.7 mm/s. Between measurements on two different solutions the channel was flushed with 500 μl deionised water. At least 3 duplicate measurements were made for each concentration. Note, fluorescence signals obtained from measurements made on quiescent Cy-5 and PI samples did not increase linearly with integration time (> 5 min), indicating photobleaching effects may be occurring at long integration times.

Prior to any on-chip fluorescence measurements, the whole optical system was properly aligned as described above. A 632.8nm (2mW He-Ne laser) was used as excitation light source for quantum dots and Cy5, while a solid state 532 nm laser was used for the PI- DNA assay. The power coming out of the tapered lens fibre was 0.5 mW and 10 mW for the 632.8 nm and 532 nm light sources respectively. The fluorescence light collected by the AWG was measured using either a TRIAX 320 spectrometer (using a 1 mm slit for quantum dot measurements and characterisation measurements, and 0.4 mm slit for Cy5 and PI measurements) or by imaging onto a 885 iXon CCD (Andor). In the latter case, for convenience, a 45° mirror was placed after AWG output channels to reflect the light into a vertically mounted camera through a ×4 objective lens (see figure 2). Here, to remove the scattered and stray light from the excitation light source, a 633nm notch filter and a 650nm long-pass filter were placed in front of the CCD for the 632.8nm laser, and a combination of 550 nm long-pass and 650nm short-pass filter was used for the 532 nm laser. The CCD was used without EM amplification and acquisition times varied from depending on the strength of the fluorescence signal and the signal/readout noise ratio desired.

CONCLUSION

We have successfully developed an on chip AWG microspectrometer-microfluidic platform and demonstrated its capability for advanced fluorescence measurements, namely, multiplex detection and quantitative fluorescence spectroscopic analysis. The platform was monolithic and integrated with multiple functions (both optical and microfluidics) in a small footprint of a few centimetres. It was coupled with an imaging detector for recording all output signals simultaneously. By evaluating against a conventional macroscopic spectrometer using several fluorescence assays, we have demonstrated that such a system can not only perform equivalent spectroscopic analysis, but offers significant advantages in multiplex detection and simplicity over on-chip solutions that employ single wavelength band filters. To the best of our knowledge, this is the first demonstration of fluorescence spectroscopic analysis using

an on chip microspectrometer monolithically integrated with a microfluidic device.

Although the current system is designed for fluorescence based detection, in principle, it can be implemented for other spectroscopic analysis, such as Raman spectroscopy. Despite the demanding requirement of the spectral resolution for Raman detection, current fabrication technology suggests it is feasible[42]. The platform can be made disposable since its fabrication can be readily scaled up using established semiconductor industry approaches. In addition, its small footprint means that it could be easily packaged with a miniaturised light source (e.g. laser diode) and imaging camera (e.g. as in a mobile phone), thereby holding great potential to create a handheld, low cost biosensor with versatile detection capability.

ACKNOWLEDGMENTS

The authors gratefully acknowledge the assistance of Gemfire Ltd (http://www.gemfire.com/) with the AWG work. Z.H thanks the support from the Chinese Council Scholarship and the University of Glasgow for his scholarship and access to the JWNC fabrication facilities. HY appreciates the financial support of the Royal Society of Edinburgh. We thank the AWG Utility from the RSoft Ltd for their assistance in the 3D BeamPROP simulation.

School of Engineering, University of Glasgow, G12 8LT Glasgow, U.K.
**Email : Huabing.Yin@glasgow.ac.uk, tel : +441413304109*

REFERENCES

1. D. N. Stratis-Cullum, G. D. Griffin, J. Mobley, A. A. Vass and T. Vo-Dinh, *Anal. Chem.*, 2003, 75, 275-280.
2. J. M. Ruano, A. Glidle, A. Cleary, A. Walmsley, J. S. Aitchison and J. M. Cooper, *Biosens. Bioelectron.*, 2003, 18, 175-184.
3. H. F. Li and J. M. Lin, *Anal. Bioanal. Chem.*, 2009, 393, 555-567.
4. D. Ivnitski, I. Abdel-Hamid, P. Atanasov and E. Wilkins, *Biosens. Bioelectron.*, 1999, 14, 599-624.
5. L. F. Capitan-Vallvey and A. J. Palma, *Anal. Chim. Acta*, 2011, 696, 27-46.
6. K. R. Rogers, *Biosens. Bioelectron.*, 1995, 10, 533-541.
7. M. Dandin, P. Abshire and E. Smela, *Lab Chip*, 2007, 7, 955-977.
8. B. Kuswandi, Nuriman, J. Huskens and W. Verboom, *Anal. Chim. Acta*, 2007, 601, 141-155.
9. F. B. Myers and L. P. Lee, *Lab Chip*, 2008, 8, 2015-2031.
10. M. A. Burns, B. N. Johnson, S. N. Brahmasandra, K. Handique, J. R. Webster, M. Krishnan, T. S. Sammarco, P. M. Man, D. Jones, D. Heldsinger, C. H. Mastrangelo and D. T. Burke, *Science*, 1998, 282, 484-487.
11. S. Balslev, A. M. Jorgensen, B. Bilenberg, K. B. Mogensen, D. Snakenborg, O. Geschke, J. P. Kutter and A. Kristensen, *Lab Chip*, 2006, 6, 213-217.
12. J. A. Chediak, Z. S. Luo, J. G. Seo, N. Cheung, L. P. Lee and T. D. Sands, *Sens. Actuator A-Phys.*, 2004, 111, 1-7.
13. E. Thrush, O. Levi, W. Ha, K. Wang, S. J. Smith and J. S. Harris, *J. Chromatogr. A*, 2003, 1013, 103-110.
14. C. Richard, A. Renaudin, V. Aimez and P. G. Charette, *Lab Chip*, 2009, 9, 1371-1376.
15. P. Measor, B. S. Phillips, A. Q. Chen, A. R. Hawkins and H. Schmidt, *Lab Chip*, 2011, 11, 899-904.
16. A. Llobera, S. Demming, H. N. Joensson, J. Vila-Planas, H. Andersson-Svahn and S. Buttgenbach, *Lab Chip*, 2010, 10, 1987-1992.
17. C. L. Bliss, J. N. McMullin and C. J. Backhouse, *Lab Chip*, 2008, 8, 143-151.
18. M. L. Adams, M. Enzelberger, S. Quake and A. Scherer, *Sens. Actuator A-Phys.*, 2003, 104, 25-31.
19. T. Vo-Dinh, J. Fetzer and A. D. Campiglia, *Talanta*, 1998, 47, 943-969.
20. M. E. Germain and M. J. Knapp, *Chem. Soc. Rev.*, 2009, 38, 2543-2555.
21. A. Chandrasekaran and M. Packirisamy, *Biomed. Microdevices*, 2010, 12, 923-933.
22. R. F. Wolffenbuttel, *IEEE Trans. Instrum. Meas.*, 2004, 53, 197-202.
23. S. Janz, A. Balakrishnan, S. Charbonneau, P. Cheben, M. Cloutier, A. Delage, K. Dossou, L. Erickson, M. Gao, P. A. Krug, B. Lamontagne, M. Packirisamy, M. Pearson and D. X. Xu, *IEEE Photonics Technol. Lett.*, 2004, 16, 503-505.
24. D. S. Goldman, P. L. White and N. C. Anheier, *Appl. Optics*, 1990, 29, 4583-4589.
25. B. Momeni, E. S. Hosseini and A. Adibi, *Opt. Express*, 2009, 17, 17060-17069.
26. B. Schauwecker, G. Przyrembel, B. Kuhlow and C. Radehaus, *IEEE Photonics Technol. Lett.*, 2000, 12, 1645-1646.
27. M. K. Smit, *Electron. Lett.*, 1988, 24, 385-386.
28. M. K. Smit and C. vanDam, *IEEE J. Sel. Top. Quantum Electron.*, 1996, 2, 236-250.
29. J. S. Kee, D. P. Poenar, P. Neuzil, L. Yobas and Y. Chen, *Opt. Express*, 2010, 18, 21732-21742.
30. K. Kodate and Y. Komai, *J. Opt. A-Pure Appl. Opt.*, 2008, 10.
31. Y. Komai, H. Nagano, K. Okamoto and K. Kodate, *Jpn. J. Appl. Phys. Part 1 - Regul. Pap. Brief Commun. Rev. Pap.*, 2006, 45, 6742-6749.
32. P. C. Ashok, G. P. Singh, H. A. Rendall, T. F. Krauss and K. Dholakia, *Lab Chip*, 2011, 11, 1262-1270.
33. R. Wilson, P. Monaghan, S. A. Bowden, J. Parnell and J. M. Cooper, *Anal. Chem.*, 2007, 79, 7036-7041.
34. K. Takada, M. Abe, M. Shibata, M. Ishii and K. Okamoto, *IEEE Photonics Technol. Lett.*, 2001, 13, 1182-1184.
35. Y. Hida, Y. Hibino, T. Kitoh, Y. Inoue, M. Itoh, T. Shibata, A. Sugita, A. Himeno and I. NTT Photonics Labs., *Electron. Lett.*, 2001, 36, 576-577.
36. M. Bruchez, M. Moronne, P. Gin, S. Weiss and A. P. Alivisatos, *Science*, 1998, 281, 2013-2016.
37. S. Rauf, A. Glidle and J. M. Cooper, *Chem. Commun.*, 2010, 46, 2814-2816.
38. C. Lodeiro, J. L. Capelo, J. C. Mejuto, E. Oliveira, H. M. Santos, B. Pedras and C. Nunez, *Chem. Soc. Rev.*, 2010, 39, 2948-2976.
39. I. Nicoletti, G. Migliorati, M. C. Pagliacci, F. Grignani and C. Riccardi, *J. Immunol. Methods*, 1991, 139, 271-279.
40. L. Strekowski and B. Wilson, *Mutat. Res.-Fundam. Mol. Mech. Mutagen.*, 2007, 623, 3-13.
41. W. D. Wilson, C. R. Krishnamoorthy, Y. H. Wang and J. C. Smith, *Biopolymers*, 1985, 24, 1941-1961.
42. N. Ismail, L. P. Choo-Smith, K. Worhoff, A. Driessen, A. C. Baclig, P. J. Caspers, G. J. Puppels, R. M. de Ridder and M. Pollnau, *Opt. Lett.*, 2011, 36, 4629-4631.